



Enhanced Suppression of First Harmonic Competing Modes in Harmonic Coaxial Gyrotron Cavities with Tapered Corrugation Depth

Lukas Feuerstein¹ · Konstantinos A. Avramidis² · Ioannis Chelis² · Benjamin Ell¹ · Stefan Illy¹ · John Jelonnek¹ · Elena Katsara² · Dimitrios Peponis² · André Schmidt¹ · Manfred Thumm¹ · Ioannis Tigelis² · Niklas Wirth¹ · Chuanren Wu¹

Received: 27 January 2026 / Accepted: 19 March 2026 / Published online: 26 March 2026
© The Author(s) 2026

Abstract

The international race toward realizing the first economically viable fusion power plant is in full progress. Start-ups, in particular, are proposing compact high-field tokamak experiments that require electron cyclotron heating at frequencies well above 200 GHz. This demand drives the intensive pursuit of high-power gyrotrons operating beyond 200 GHz. Second harmonic operation offers a promising route to reach such frequencies without necessitating stronger magnetic fields. However, the intrinsically lower interaction efficiency and strong competition from first harmonic modes pose significant challenges. To enhance mode selectivity, we propose a cavity design with a novel scheme of profiled impedance corrugations, changing the surface impedance on the inner conductor along the axis of a coaxial gyrotron cavity. This design achieves unprecedented suppression of competing first harmonic modes while maintaining ohmic wall loading levels compatible with continuous-wave (CW) operation. As a result, this novel corrugation scheme enables higher output power, broadens the range of stable gyrotron operation, and substantially reduces sensitivity to electron beam quality. These advances establish tapered impedance corrugations as a powerful tool for realizing robust, efficient, and scalable harmonic gyrotrons at sub-terahertz frequencies.

Keywords Electron tubes · Gyrotrons · Coaxial resonators · Corrugated insert · Second harmonic operation

✉ Lukas Feuerstein
lukas.feuerstein@kit.edu

¹ Institute for Pulsed Power and Microwave Technology, Karlsruhe Institute of Technology, Hermann-von-Helmholtz-Platz 1, 76344 Eggenstein-Leopoldshafen, Germany

² Department of Physics, National and Kapodistrian University of Athens, 15784 Athens, Greece

1 Introduction

Gyro-devices operate based on the electron cyclotron resonance effect [1]. Thus, the angular frequency ω of the generated microwave is close to the electron cyclotron frequency Ω_c of the electrons or higher harmonics thereof. The interaction condition between electrons and the electric field at any harmonic s can be expressed as

$$\omega \approx s \Omega_c + k_z v_z, \quad (1)$$

where k_z denotes the axial wave number and v_z the axial electron velocity. As Ω_c is proportional to the static magnetic flux density B_z , the output frequency can be doubled with the same magnetic flux density when utilizing second harmonic interaction.

Fusion gyrotrons, unlike harmonic gyrotrons for dynamic nuclear polarization spectroscopy as presented in [2–4], demand MW-level microwave output power, and therefore utilize highly overmoded cavities to minimize wall losses. However, when targeting second harmonic operation ($s = 2$), this design leads to strong competition from first harmonic modes whose cutoff frequencies are close to the cyclotron frequency. Thus, to enable efficient harmonic interaction, the cavity must be designed to prevent excitation of these first harmonic modes.

The most promising approaches for harmonic MW-level gyrotron cavities include the use of an external injection signal, which forces the electrons to interact at a specific frequency [5], or the targeted suppression of first harmonic competing modes by means of a coaxial cavity. Such cavities feature an impedance-corrugated inner conductor combined either with outer mode-converting corrugations [6] or with smooth outer cavity walls [7, 8]. Other alternative methods, like the use of resistive, up-tapered inner conductors, are difficult to apply for MW-class gyrotrons due to the high ohmic load on the inner conductor [9].

Suppressing first harmonic modes via an injection signal offers the added benefit of frequency locking to a master oscillator. However, the injection power is not negligible compared to the output signal. As shown theoretically in [10, 11], as well as in gyrotron interaction simulations in [12], the required locking power follows Adler's relation [13]. Consequently, to achieve output powers exceeding 1 MW at an operating frequency of 170 GHz—using a cavity with a moderate diffractive quality factor of $Q = 1500$ —an injection power of at least 100–200 kW is required. This ensures an adequate locking bandwidth of approximately ± 30 MHz, sufficient to compensate for manufacturing tolerances on the order of ± 5 μm . Therefore, to deliver the necessary injection-locking power, a medium-power gyrotron would be needed as the master oscillator, as described in [14]. Additionally, methods must be employed to stabilize the master oscillator [15] and to tune the resonance frequency of the master oscillator to compensate the frequency shift due to thermal expansion of the cavity. Therefore, the use of injection locking involves considerable effort.

Compared to the injection-locking approach, the possibility of suppressing first harmonic modes using an impedance-corrugated inner conductor would simplify the layout for electron cyclotron resonance heating (ECRH) installations at frequencies above 250 GHz, where second harmonic gyrotrons can be advantageous.

This article considers the possibility of suppressing first harmonic modes using an impedance-corrugated inner conductor and discusses improved first harmonic suppression by tapering the depth of corrugation on the inner conductor. This approach leads to more stable operation of the gyrotron and reduces the susceptibility to electron beam parameter tolerances.

The paper is structured as follows: Sect. 2.1 presents the theoretical basis for suppressing first harmonic competing modes in cavities equipped with coaxial inserts featuring constant-depth corrugations. Section 2.2 details the underlying principles and design methodology of the proposed approach, which involves a tapered corrugation depth on the inner conductor. A representative numerical design is provided in Sect. 3 for a 170 GHz second harmonic $TE_{34,19}$ coaxial cavity incorporating tapered corrugations on the coaxial insert. To evaluate the effectiveness of the proposed method, tolerance analyses are conducted for various beam parameters that may impact the performance of the second harmonic $TE_{34,19}$ operating mode.

2 Suppression Scheme for First Harmonic Competing Modes

Unlike in a hollow cavity, the eigenvalue χ of a TE mode in a coaxial cavity is geometry-dependent. The eigenmodes of coaxial cavities are influenced by the ratio of the outer to inner wall radii, following denoted by C . Thus, the cutoff frequency and diffractive quality factor can be influenced not only by the geometry of the outer wall but also by the shape of the inner conductor within the cavity. As a result, competing modes with smaller caustic radii than the operating mode can be effectively suppressed. This suppression can be further enhanced by introducing longitudinal corrugations on the inner conductor [16].

2.1 Coaxial Gyrotron Cavities with Constant Corrugation Depth

If the period of the corrugations along the circumference of the coaxial insert is significantly smaller than half of the free-space wavelength λ and the number of corrugations satisfies $N > |m| + \chi$, where m is the azimuthal mode order of the $TE_{m,n}$ mode, azimuthal mode conversion due to the corrugations can be neglected [17]. In this regime, the corrugations can be described by an effective surface impedance model (SIM). For SIM corrugated coaxial cavities, the eigenvalue χ of the mode $TE_{m,n}$, depends not only on the ratio of the outer to inner cavity wall radii $C = r_{\text{out}}/r_{\text{in}}$, but also on the corrugation depth d of the impedance corrugations. The eigenvalue of the coaxial eigenmode can be obtained as the roots of the characteristic equation

$$J'_m(\chi) \left(Y'_m\left(\frac{\chi}{C}\right) + w Y_m\left(\frac{\chi}{C}\right) \right) - Y'_m(\chi) \left(J'_m\left(\frac{\chi}{C}\right) + w J_m\left(\frac{\chi}{C}\right) \right) = 0, \quad (2)$$

as described in [16], where $w = l/p \tan(d/r_{\text{out}} \chi)$, for a corrugation width l and a period of the corrugations p . Here, J_m and Y_m denote the Bessel functions of the first

and second kind. This concept has already been successfully demonstrated in first harmonic coaxial gyrotrons [18], where d is usually chosen to be $\approx 0.25\lambda$ to suppress competing cavity modes [19]. The dependence of χ to C and d is illustrated in Fig. 1 for a corrugation width to period ratio l/p of 0.5.

While the eigenvalue approaches that of the hollow wave-guide mode for large C , and tends to infinity as $C \rightarrow 0$, it is particularly influenced by the impedance corrugations in certain regions of the eigenvalue curve. This effect is clearly visible in Fig. 1, where the eigenvalues of the coaxial $TE_{17,10}$ mode are shown for corrugation depths ranging from $d = 0\lambda$ to 0.4λ . For large corrugation depths, the eigenvalue of the $TE_{m,n}$ mode approaches that of the hollow cavity eigenvalue corresponding to the $TE_{m,n-1}$ mode.

For second harmonic operation, d is chosen to be between 0.4λ and 0.6λ of the operating mode. While the corrugations present a low surface impedance for the second harmonic operating mode, the first harmonic competing modes are presented a high surface impedance. In combination with a down-tapered inner conductor radius, the eigenvalue of the first harmonic competing modes decreases along the cavity, if the inner conductor radius is carefully selected. This effect is illustrated in Fig. 2, where it results in a reduced diffractive quality factor Q , and consequently, an increased starting current for the affected modes. For instance, the Q of the $TE_{17,10}$ mode, the main first harmonic competing mode to the second harmonic operating mode $TE_{34,19}$,

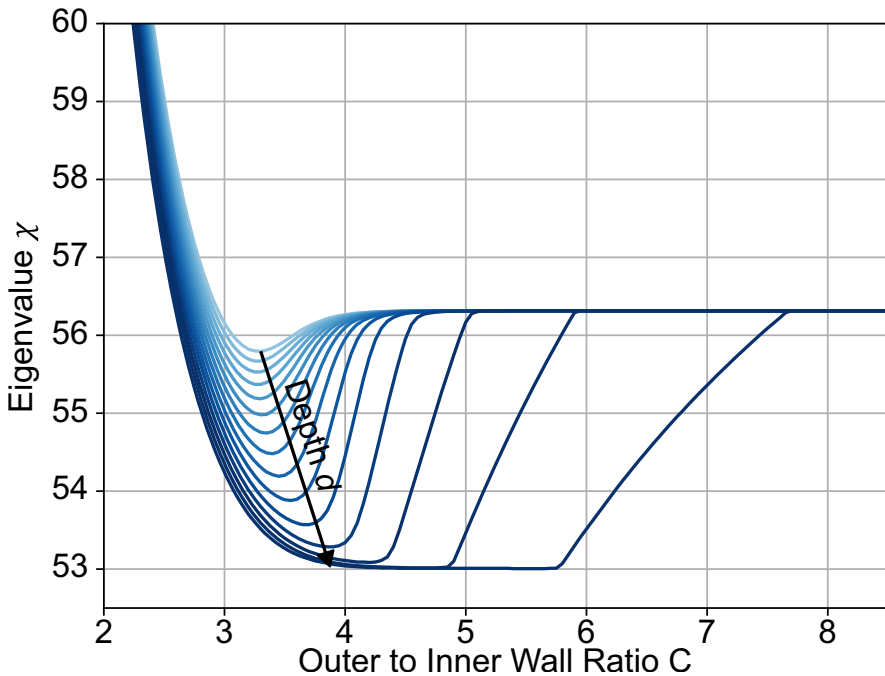


Fig. 1 Eigenvalue of the most critical first harmonic competing mode $TE_{17,10}$ for corrugation depth of $d = 0.0\lambda$ to 0.4λ in 15 steps for an outer wall radius of $r_{\text{out}} = 29.55$ mm, a corrugation width of 0.3 mm and a corrugation period of 0.6 mm

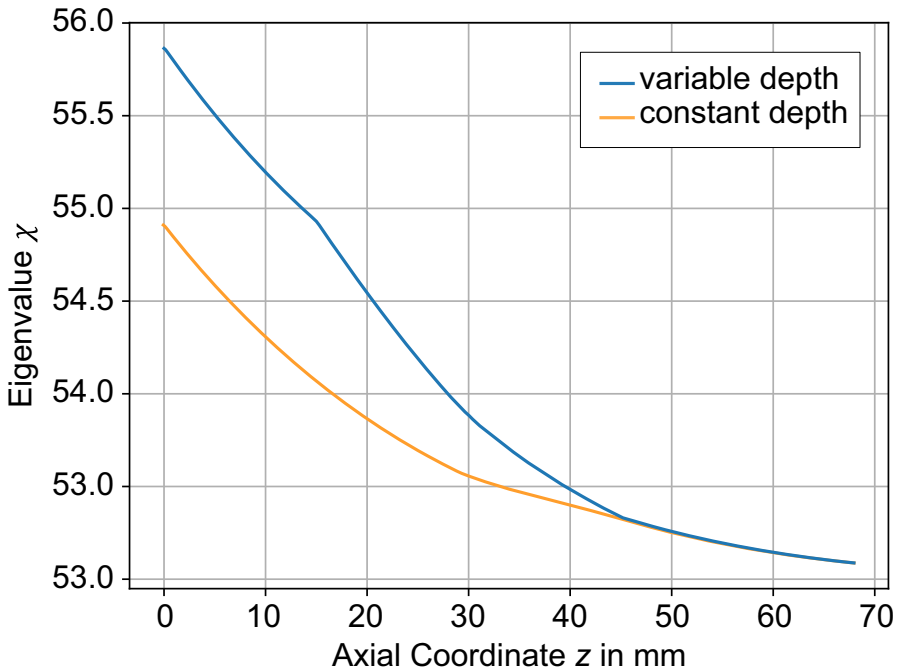


Fig. 2 Eigenvalue of the most critical first harmonic competing mode $TE_{17,10}$ versus cavity axial coordinate with constant and with profiled corrugation depth

can be decreased from $Q = 957$ to $Q = 495$ solely by employing the SIM corrugated coaxial insert, compared to a hollow cavity with an identical outer radius contour. This approach can be employed in the design of a second harmonic coaxial gyrotron capable of delivering output powers of up to 1.6 MW, as detailed in [7, 8].

Nevertheless, to achieve a sufficient suppression of the first harmonic competing modes, the radius of the coaxial insert of a second harmonic gyrotron has to be larger than the radius of the coaxial insert of a fundamental coaxial gyrotron with the same operating mode. This increases the ohmic wall loading on the insert, which should be below 0.39 kW/cm^2 [20]. Also, the second harmonic interaction is more prone to beam parameter tolerances. To make the operation of the gyrotron more robust, further methods have to be found to enhance the cavity design.

2.2 Axially Profiled Corrugation Depth

To further enhance the suppression of competing modes, their diffractive quality factor must be reduced even further [21]. As illustrated in Fig. 1, the eigenvalue of the $TE_{m,n}$ mode can be decreased to the eigenvalue of the hollow $TE_{m,n-1}$ mode by increasing the corrugation depth d . Varying d —and thereby the effective surface impedance of the inner conductor—can change the eigenvalue of the first harmonic competing mode even for a constant outer to inner wall ratio. This results in a comparable impact on the diffractive quality factor as tapering the inner conductor. A preliminary theoret-

ical investigation into axially distributed stepped corrugation depths was previously proposed for DNP gyrotrons [22]. However, to enable practical implementation in high-power gyrotrons, a more robust and manufacturable design approach remains necessary.

Since χ is more sensitive to d , than to C in the region of the eigenvalue curve where χ is most affected, keeping C constant and modifying d demands high manufacturing precision, both in milling the impedance corrugations and in positioning the coaxial insert. The tolerances can be relaxed by simultaneously varying both C and d . For the physical implementation, this implies tapering the insert radius and corrugation depth along the cavity axis, thereby distributing the eigenvalue reduction over a larger axial region. As the corrugation depth increases, the range of C where $\chi_{m,n}$ approaches $\chi_{m,n-1}$ can be enlarged. Following, it is possible to decrease the coaxial insert radius while still influencing the first harmonic competing modes. With a decreased coaxial insert radius, the ohmic loading on the coaxial insert can also be reduced.

In contrast to other conceivable profiles of d that would increase the suppression of first harmonic competing modes, such as a stepwise increase in C to enhance d , a simultaneous taper of both C and d can be readily manufactured mechanically. Such a profile can be fabricated using disk cutters or 5-axis CNC machining, analogous to the coaxial inserts previously produced for the first harmonic coaxial gyrotron at the Karlsruhe Institute of Technology [23]. In particular, for the disk-cutting manufacturing method, the rounding at the bottom of the corrugations is sufficiently small to be neglected. Large roundings at the corrugation bottom would result in a shift of the effective corrugation depth and therefore the effective surface impedance. The tolerance of the corrugation depth is comparable to that of well-established constant-depth designs.

The design should avoid the region of the eigenvalue curve, in which the so-called inner mode appears, as it may lead to field elevation at the insert [17, 24]. Additionally, the transition to the inner mode poses the risk of coupling between the $TE_{m,n}$ and $TE_{m,n-1}$ modes, due to the convergence of their respective eigenvalues within this region. This imposes constraints on the minimum allowable value of d at the entrance of the cavity. Furthermore, the region of low C , with strongly increasing χ , should be avoided, as this could adversely affect the operating mode.

To influence χ , in addition to adjusting d , the ratio l/p along the cavity could also be varied. However, this approach presents manufacturing challenges, as l is determined by the thickness of the milling cutter used, and p depends on the number of corrugations distributed along the circumference of the coaxial insert. Consequently, this method is generally not preferred. The variation of p along the length of the cavity due to the taper of the coaxial insert is negligible for small taper angles.

3 Numerical Design of a Coaxial Gyrotron Cavity with Profiled Corrugations

To validate the proposed method, a cavity design optimized for second harmonic operation was developed based on the coaxial $TE_{34,19}$ 170 GHz gyrotron from [23]. The cavity was designed to match the mechanical interfaces of the existing coaxial KIT

shortpulse prototype. In the following, the cavity is compared in two configurations: one with a constant corrugation depth of the coaxial insert at 0.4λ (Case I), and another one with a tapered insert corrugation, as shown in Fig. 3 (Case II). The interaction simulations were carried out using the new KIT self-consistent, time-dependent interaction codes ROCK [25], based on modeling the electron movement in cyclotron coordinates, as well as the PIC code simpleRick [26]. Both codes are able to simulate the electron-wave interaction of impedance-corrugated coaxial gyrotron cavities and show comparable results for simulations presented in the following section.

The cavity has an outer radius of 29.55 mm with 3.0° downtaper and 2.5° uptaper angle. The constant midsection length is 20 mm with 6 mm parabolic roundings. The inner conductor has an outer radius of 8.5 mm and is downtapered with 2.5° along the cavity axis.

For Case II, additionally, the corrugation depth is increased from 0.5 to 0.71 mm in an axial region from $z = 19 - 53$ mm, as presented in Fig. 3.

The eigenvalue of the primary first harmonic competing mode $TE_{17,10}$ along the axis for both cases is shown in Fig. 2. It becomes evident that in the case of profiled corrugations, the eigenvalue decreases more significantly along the cavity axis than in the case of constant corrugations—particularly in the region of the constant midsection from $z = 19 - 45$ mm. This leads to a further reduction of the cold diffractive quality factor from 495 in Case I to 297 in Case II of the $TE_{17,10}$ competing mode.

In both cases, time-dependent multimode interaction simulations with up to 95 competing modes yield an output power of 1.3 MW in second harmonic opera-

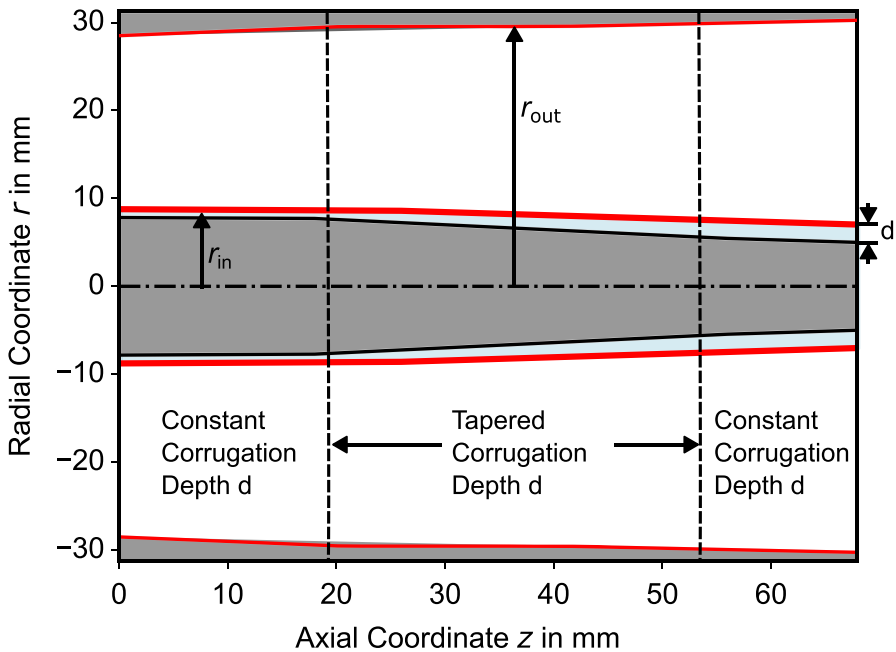


Fig. 3 Schematic cross-section of the coaxial $TE_{34,19}$ cavity with tapered impedance corrugations

Table 1 Operating parameters

Electron kinetic energy E_{kin}	90 keV
Beam current I_b	70 A
Pitch factor α	1.3
Guiding center radius r_{gc}	9.62 mm
Magnetic field B_z	3.5 T
Pitch factor spread $\delta\alpha$	8 %
Guiding center spread δr_{gc}	0.8 %
Kinetic energy spread δE_{kin}	0.02 %

tion, with an interaction efficiency of 21 % at the operating point shown in Table 1. The selected operating point is compatible with the triode gun from [27] and keeps a margin of 2 kV to the point of mode loss. Since the energy spectrum of the electron beam is less spread out after the cavity compared to first harmonic operation, the use of a multi-stage depressed collector, as demonstrated in [28], can significantly increase the overall efficiency of the gyrotron.

To highlight the effectiveness of the profiled inner corrugations, sensitivity studies have been performed. In these investigations, Case I and Case II have been simulated quasistationary, with constant beam parameters for 300 ns of simulation time, for different pitch factors α , while all other beam parameters have been kept unchanged. Each datapoint of Fig. 4a and b refers to such a quasistationary simulation. In the cavity with constant corrugation depth, the second harmonic operating mode could only be excited in a range of $\alpha = 1.1 - 1.3$, as shown in Fig. 4a. For $\alpha > 1.3$, the first harmonic competing mode TE_{17,10} starts to prevail. In the profiled corrugated Case II, the second harmonic mode could be excited up to a pitch factor of $\alpha = 1.8$ as it can be seen in Fig. 4b.

Similar studies were performed with regard to other beam parameters, such as the beam current. In Case II, the second harmonic mode remains excitable up to a beam

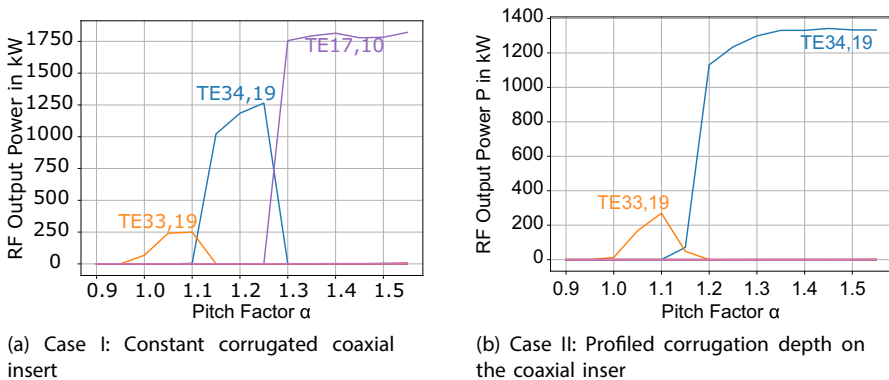


Fig. 4 Quasistationary simulated output power of the second harmonic cavity with constant corrugated coaxial insert (Case I) and with profiled corrugation depth on the coaxial insert (Case II) at the operating point listed in Table 1

current of 100 A and 1.9 MW of output power, while maintaining the ohmic wall limit of 2.5 kW/cm^2 on the outer wall and 0.39 kW/cm^2 on the inner cavity wall [20]. For beam currents above 100 A, the competing modes suppress the second harmonic operating mode.

To evaluate the acceptable beam misalignment, which may occur in experiments due to a mismatch between the cavity axis and the magnetic axis, the electron beam was intentionally displaced in the interaction simulations using the PIC code SIMPLERICK. The numerical results indicate that the second harmonic operating modes can still be excited with misalignments of up to 0.6 mm. In this case, the output power is reduced to 500 kW as shown in Fig. 5.

For larger misalignments, the operating mode is suppressed by competing modes. These tolerances are comparable to those of the fundamental gyrotron studied in [23], and can be compensated by employing dipole coils in the magnetic system.

Due to the better suppression of the competing modes, it is also possible to decrease the insert radius. This reduces the ohmic loading on the coaxial insert and increases the clearance between the inner cavity wall and electron beam. For the constant corrugated insert, the main first harmonic competitor $\text{TE}_{17,10}$ suppresses the second harmonic interaction, if the insert radius is below 8.3 mm. For the cavity of Case II, the radius can be reduced to 7.9 mm, while maintaining the second harmonic operating mode.

This scheme of profiled surface impedance corrugations can also be utilized to design coaxial gyrotron cavities with operating frequencies of 280 GHz with still manufacturable corrugation sizes and tolerances [29].

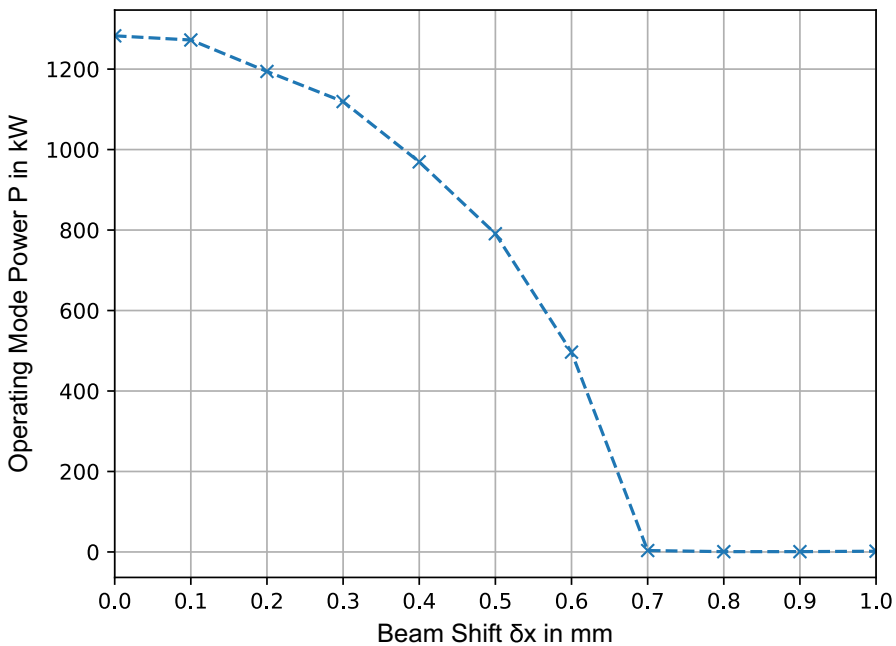


Fig. 5 Maximum power of the main mode $\text{TE}_{34,19}$ versus the beam misalignments δx

4 Conclusions

This work presents a novel approach to enhance mode selectivity in coaxial high-power gyrotrons by introducing a tapered corrugation depth along the coaxial insert. This technique is particularly advantageous for high-power second harmonic gyrotrons, where strong competition from first harmonic modes arises. Through detailed theoretical analysis and interaction simulations, we demonstrate that this approach significantly reduces the diffractive quality factor Q of first harmonic competing modes while preserving the high performance of the desired second harmonic mode.

The proposed design allows for a reduction in the insert radius, leading to decreased ohmic loading on the inner cavity wall and improved beam clearance. Moreover, the tapered configuration was shown to increase the operational tolerance against variations in beam parameters such as pitch factor and current, thereby improving the robustness of the cavity.

Compared to constant-depth corrugated designs, the tapered structure extends the stable operating range and enables higher output power without sacrificing efficiency. These improvements are validated through multimode interaction simulations using self-consistent time-dependent multimode codes, showing output powers exceeding 1.3 MW and interaction efficiencies of over 21 %.

These findings contribute a promising pathway toward the design of more stable and efficient second harmonic, high-frequency, high-power gyrotrons, which could enable ECRH applications for frequencies significantly above 200 GHz at reasonable cost.

Acknowledgements This work has been carried out within the framework of the EUROfusion Consortium, funded by the European Union via the Euratom Research and Training Programme (Grant Agreement No 101052200 – EUROfusion). Views and opinions expressed are, however, those of the author(s) only and do not necessarily reflect those of the European Union or the European Commission. Neither the European Union nor the European Commission can be held responsible for them. The authors affiliated with KIT acknowledge support by the state of BadenWürttemberg through bwHPC. We acknowledge support by the KIT-Publication Fund of the Karlsruhe Institute of Technology.

Author Contributions L. Feuerstein, S. Illy, and J. Jelonnek wrote the main manuscript. I. Tigelis and M. Thumm provided scientific consulting and project oversight. K.A. Avramides, I. Chelis, E. Katsara, D. Peponis, and A. Schmidt contributed to the theoretical considerations of coaxial second harmonic gyrotrons. L. Feuerstein, B. Ell, and C. Wu contributed to the numerical design. N. Wirth prepared the considerations on mechanical limits and manufacturability. All authors reviewed the manuscript.

Funding Open Access funding enabled and organized by Projekt DEAL. This work has been funded by the European Union via the Euratom Research and Training Programme (Grant Agreement No 101052200 – EUROfusion).

Data Availability No datasets were generated or analysed during the current study.

Declarations

Ethical Approval Not applicable.

Competing Interests The authors declare no competing interests.

Open Access This article is licensed under a Creative Commons Attribution 4.0 International License, which permits use, sharing, adaptation, distribution and reproduction in any medium or format, as long as you give appropriate credit to the original author(s) and the source, provide a link to the Creative Commons licence, and indicate if changes were made. The images or other third party material in this article are included in the article's Creative Commons licence, unless indicated otherwise in a credit line to the material. If material is not included in the article's Creative Commons licence and your intended use is not permitted by statutory regulation or exceeds the permitted use, you will need to obtain permission directly from the copyright holder. To view a copy of this licence, visit <http://creativecommons.org/licenses/by/4.0/>.

References

1. Flyagin, V.A., et al.: The Gyrotron. *IEEE Transactions on Microwave Theory and Techniques* 25(6), 514–521 (1977) <https://doi.org/10.1109/TMTT.1977.1129149>
2. Bandurkin, I.V., et al.: Development of Second-Harmonic Terahertz Gyrotrons with Highly Selective Cavities. In: 50th European Microwave Conference (EuMC), pp. 603–606 (2021). <https://doi.org/10.23919/EuMC48046.2021.9338035>
3. Idehara, T., et al.: A novel THz-band double-beam gyrotron for high-field DNP-NMR spectroscopy. *Review of Scientific Instruments* 88(9), 094708 (2017) <https://doi.org/10.1063/1.4997994>
4. Shcherbinin, V.I., Tkachenko, V.I.: Cylindrical Cavity with Distributed Longitudinal Corrugations for Second-Harmonic Gyrotrons. *J Infrared Milli Terahz Waves* 38(7), 838–852 (2017) <https://doi.org/10.1007/s10762-017-0386-x>
5. Denisov, G.G., et al.: Phase-Locking of Second-Harmonic Gyrotrons for Providing MW-Level Output Power. *IEEE Transactions on Electron Devices*, 1–5 (2021) <https://doi.org/10.1109/TED.2021.3134187>
6. Peponis, D.V., et al.: Design of MW-Class Coaxial Gyrotron Cavities With Mode-Converting Corrugation Operating at the Second Cyclotron Harmonic. *IEEE Transactions on Electron Devices* 70(12), 6587–6593 (2023) <https://doi.org/10.1109/TED.2023.3326431>
7. Feuerstein, L., et al.: Design of a Second Harmonic MW-Level Coaxial Gyrotron Cavity. In: 24th International Vacuum Electronics Conference (IVEC), pp. 1–2 (2023). <https://doi.org/10.1109/IVEC56627.2023.10156958>
8. Chelis, I.G., et al.: High-Frequency MW-class Coaxial Gyrotron Cavities Operating at the Second Cyclotron Harmonic. *IEEE Transactions on Electron Devices*, 1–7 (2024) <https://doi.org/10.1109/TED.2024.3356472>
9. Avramides, K.A., Vomvoridis, J.L., Iatrou, C.T.: Coaxial Gyrotron Cavities with Resistive Corrugated Insert for Powerful Second-Harmonic Operation. *AIP Conference Proceedings* 807(1), 264–270 (2006) <https://doi.org/10.1063/1.2158787>
10. Jelonnek, J.: Untersuchung des Lastverhaltens von Gyrotrons. PhD thesis, Technischen Universität Hamburg-Harburg, Hamburg (2000)
11. Sabchevski, S.: Parallels Between Models of Gyrotron Physics and Some Famous Equations Used in Other Scientific Fields. *Applied Sciences* 15(14), 7920 (2025) <https://doi.org/10.3390/app15147920>
12. Brücker, P., Avramidis, K.A., Marek, A., Thumm, M., Jelonnek, J.: Theoretical Investigation on Injection Locking of the EU 170 GHz 2 MW TE_{34,19}-Mode Coaxial-Cavity Gyrotron. In: 46th International Conference on Infrared, Millimeter and Terahertz Waves (IRMMW-THz), pp. 1–2 (2021). <https://doi.org/10.1109/IRMMW-THz50926.2021.9567563>
13. Adler, R.: A Study of Locking Phenomena in Oscillators. *Proceedings of the IRE* 34(6), 351–357 (1946) <https://doi.org/10.1109/JRPROC.1946.229930>
14. Bakunin, V.L., et al.: An Experimental Study of the External-Signal Influence on the Oscillation Regime of a Megawatt Gyrotron. *Radiophysics and Quantum Electronics* 62(7), 481–489 (2019) <https://doi.org/10.1007/s11141-020-09994-y>
15. Fokin, A.P., et al.: First Experiments on Frequency Locked Operation of the 170GHz/1MW Gyrotron. In: *Photonics & Electromagnetics Research Symposium (PIERS)*, pp. 1–6 (2024). <https://doi.org/10.1109/PIERS62282.2024.10618801>
16. Iatrou, C.T., Kern, S., Paveleyev, A.B.: Coaxial cavities with corrugated inner conductor for gyrotrons. *IEEE Transactions on Microwave Theory and Techniques* 44(1), 56–64 (1996) <https://doi.org/10.1109/22.481385>

17. Ioannidis, Z.C., Avramides, K.A., Latsas, G.P., Tigelis, I.G.: Azimuthal Mode Coupling in Coaxial Waveguides and Cavities With Longitudinally Corrugated Insert. *IEEE Transactions on Plasma Science* 39(5), 1213–1221 (2011) <https://doi.org/10.1109/TPS.2011.2118766>
18. Piosczyk, B., et al.: A 1.5-MW, 140-GHz, TE_{28,16}-coaxial cavity gyrotron. *IEEE Transactions on Plasma Science* 25(3), 460–469 (1997) <https://doi.org/10.1109/27.597261>
19. Kern, S.: Numerische Simulation der Gyrotron-Wechselwirkung in koaxialen Resonatoren. PhD thesis, Forschungszentrum Karlsruhe, Karlsruhe (1996)
20. Kalaria, P.C., George, M., Illy, S., Avramidis, K.A., Gantenbein, G., Ruess, S., Thumm, M., Jelonnek, J.: Multiphysics Modeling of Insert Cooling System for a 170-GHz, 2-MW Long-Pulse Coaxial-Cavity Gyrotron. *IEEE Transactions on Electron Devices* 66(9), 4008–4015 (2019) <https://doi.org/10.1109/TED.2019.2928222>
21. Dumbrajs, O.: Novel method of improving performance of coaxial gyrotron resonators. *IEEE Transactions on Plasma Science* 30(3), 836–839 (2002) <https://doi.org/10.1109/TPS.2002.801605>
22. Shcherbinin, V.I.: Multifunctional Coaxial Insert With Distributed Impedance Corrugations for Cavities of Broadband Tunable Second-Harmonic Gyrotrons. *IEEE Transactions on Electron Devices* 68(8), 4104–4109 (2021) <https://doi.org/10.1109/TED.2021.3090348>
23. Ruess, T., et al.: Theoretical Study on the Operation of the EU/KIT TE_{34,19}-Mode Coaxial-Cavity Gyrotron at 170/204/238 GHz. *EPJ Web of Conferences* 203, 04014 (2019) <https://doi.org/10.1051/epjconf/201920304014>
24. Franck, J.: Systematic Study of Key Components for a Coaxial-Cavity Gyrotron for DEMO. PhD thesis, Karlsruher Forschungsberichte aus dem Institut für Hochleistungsimpuls- und Mikrowellentechnik (2017)
25. Wu, C., Feuerstein, L., Schmidt, A., Illy, S., Thumm, M., Jelonnek, J.: ROCK: A Flexible Gyrotron Cavity Simulation Toolkit Using an Accuracy-Improved Time-Dependent Self-Consistent Multimode Interaction Model. *Journal of Infrared, Millimeter, and Terahertz Waves* 46(7), 50 (2025) <https://doi.org/10.1007/s10762-025-01065-5>
26. Feuerstein, L., et al.: Validation of a New Fast-Time Scale Code for Advanced Simulations of Gyrotron Cavities. In: 14th German Microwave Conference (GeMiC), pp. 144–147 (2022)
27. Pagonakis, I.G., et al.: Triode magnetron injection gun for the KIT 2 MW 170 GHz coaxial cavity gyrotron. *Physics of Plasmas* 27(2), 023105 (2020) <https://doi.org/10.1063/1.5132615>. Accessed 2022-11-02
28. Ell, B., Feuerstein, L., Gantenbein, G., Illy, S., Ruess, T., Rzesnicki, T., Stanculovic, S., Thumm, M., Weggen, J., Wu, C., Jelonnek, J.: Robustness of the $E \times B$ MDC prototype design for gyrotrons. *Fusion Engineering and Design* 215, 114979 (2025) <https://doi.org/10.1016/j.fusengdes.2025.114979>
29. Feuerstein, L., et al.: MW Level 280 GHz 2nd Harmonic Coaxial Gyrotron Cavity with Variable Corrugation Depth. In: Joint International Vacuum Electronics Conference and International Vacuum Electron Sources Conference (IVEC + IVESC), pp. 01–02. IEEE, Monterey, CA, USA (2024). <https://doi.org/10.1109/IVECIVESC60838.2024.10694886>

Publisher's Note Springer Nature remains neutral with regard to jurisdictional claims in published maps and institutional affiliations.